

# A mathematical model of the regulation of OHC basolateral permeability and transducer operating point

Greg O'Beirne

The Auditory Laboratory, Physiology  
University of Western Australia

Dept. of Communication Disorders  
University of Canterbury

Robert Patuzzi

The Auditory Laboratory, Physiology  
University of Western Australia



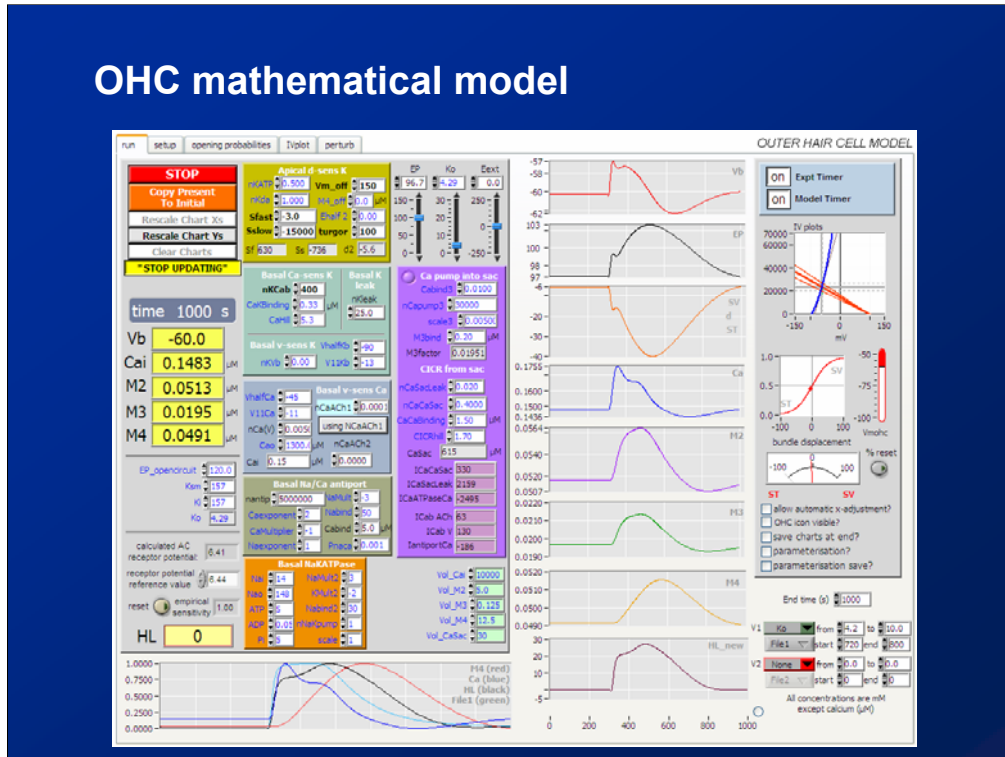
THE UNIVERSITY OF  
WESTERN AUSTRALIA



Good morning, my name is Greg O'Beirne. I'm currently at the Department of Communication Disorders at the University of Canterbury, New Zealand, but this morning I'm going to be talking about the work I have done at the University of Western Australia with Dr Robert Patuzzi, to develop a **mathematical model** of the regulation of cochlear amplification by the outer hair cells.

The mathematical model was developed as part of my PhD work, which has investigated cochlear regulation using a **combination** of mathematical modelling of the **ionic** and **mechanical** interactions likely to exist within OHCs, and electrophysiological **experiments** conducted in guinea pigs.

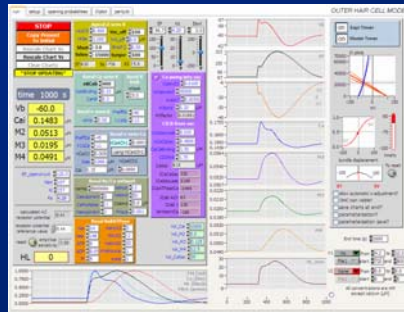
# OHC mathematical model



The mathematic model was created in an attempt to explain within **one framework** the results obtained from a **range of experiments** on cochlear regulation.

## OHC mathematical model

- incorporates known OHC electrophysiology
- includes effect of motility on apical conductance
- simulates perturbations by systematic and timed variation of one or more model parameters
- predicts changes in active gain due to OHCs
- provides a plausible and consistent explanation for **slow oscillatory behaviour** observed in the cochlea



It was clear from the outset that for such a model to provide **realistic predictions** of experimental data, it must incorporate not only what is known about the **electrophysiology** of the OHCs, but also must include their **motile properties**, as this motility directly influences the conductance at the apical membrane of the cell. The model can be used to **predict** the response of these hair cells to given experimental **perturbations**, and allows examination of the **time-course** of subsequent changes in basolateral membrane potential, ionic fluxes and concentrations, and the operating point of the MET channels.

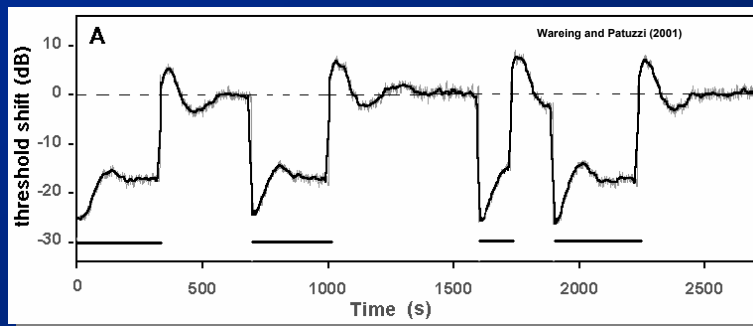
Predictions of the changes to the **active gain** of the cochlea are also generated, under the assumption that the **force-generation ability** of an outer hair cell is largely dependent on the **drive of prestin** by the small-signal AC receptor potential.

To provide some background: our work on this topic began when we were analysing the extremely slow oscillations that occur in the mammalian cochlea, and by “extremely slow” I mean a cycle time of minutes. These oscillations come in many varieties, but the best known example of this...

## The bounce phenomenon

LF stimulation causes cochlear oscillations that are measurable in:

- **Neural threshold** (Hirsch and Ward, 1952; Hughes, 1954; Hirsch and Bilger, 1955; Zwicker and Hesse, 1984; Patuzzi and Wareing, 2002)



...is the so-called “**bounce phenomenon**”, whereby exposure to an intense low-frequency tone elicits oscillations in a **number of measures** of cochlear function.

These oscillations have been found to be *mechanical* (rather than strictly neural) in origin, and are visible in measures of:

- i) **CAP thresholds** in guinea pigs and **psychophysical threshold** in humans (as shown here in this example of Bekesy audiometry, where you can see that the low-frequency exposure actually **improves** auditory thresholds transiently by about 5 dB.

## The bounce phenomenon

LF stimulation causes cochlear oscillations that are measurable in:

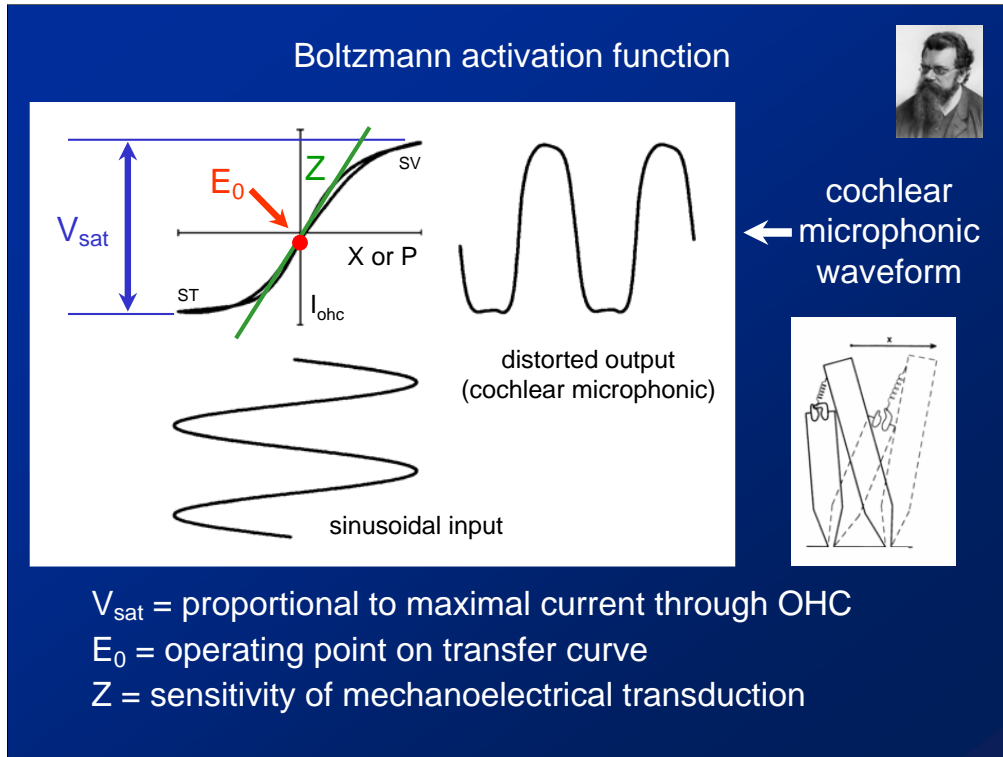
- **Neural threshold** (Hirsch and Ward, 1952; Hughes, 1954; Hirsch and Bilger, 1955; Zwicker and Hesse, 1984; Patuzzi and Wareing, 2002)
- **TEOAEs** (Kemp, 1982; 1986; Kevanishvili et al., IEB 2005)
- **$f_2$ - $f_1$  DPOAEs** (Kirk and Patuzzi, 1997)
- **EP** (Kirk, 1972; Kirk and Patuzzi, 1997; Salt, 2004)
- **Psychophysical measures of tinnitus** (Kemp, 1986; Wareing, 2001; Patuzzi and Wareing, 2002).
- **Boltzmann parameters extracted from LF CM waveforms**  
(Kirk et al., 1997)

ii) It's also visible in **transient** and **distortion-product** otoacoustic emissions

iii) the **endocochlear potential**

iv) measures of transient **tinnitus** in humans

and v) in measures of outer hair cell **mechano-electrical transduction**, such as **Boltzmann analysis** of the low-frequency cochlear microphonic waveform.



For those who are unfamiliar with Boltzmann analysis, it is a technique whereby an intense, non-traumatic, low-frequency tone (for example, around 200 Hz) is used to drive the basal-turn OHCs into partial saturation, enabling us to use a curve-fitting process to analyse the characteristics of the nonlinear transfer curve.

The parameters we extract are:

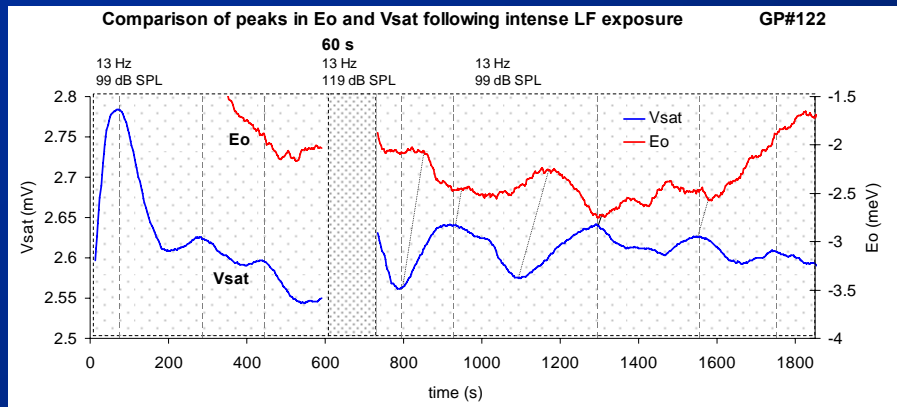
**$V_{\text{sat}}$**  – which gives the maximal current through the OHC (dominated by the cell’s basolateral permeability)

the **operating point** –  $E_0$  – which provides an indication of the resting angle of the stereocilia, which is partially determined by the degree of contraction or elongation of the hair cell; and

**$Z$**  – the overall sensitivity of the mechano-electrical transduction process.

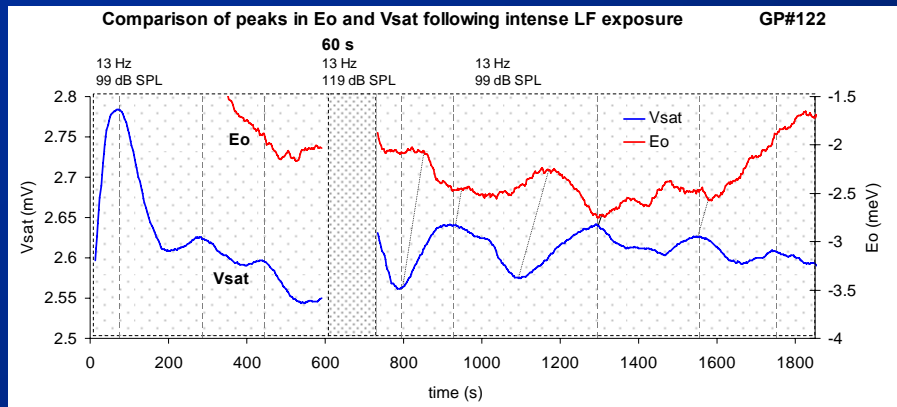
The technique allows us to probe changes in the basal-turn OHCs over several hours.

## Boltzmann parameters following LF exposure



Now, if we look at two of these Boltzmann parameters recorded during exposure to a very-low-frequency tone (around 13 Hz), we see that these **slow oscillations** are visible in our measures of basolateral permeability (shown here in blue) and operating point (shown in red). The time scale along here is 30 minutes.

## Boltzmann parameters following LF exposure



- OHC basolateral permeability ( $V_{sat}$ ) and operating point ( $E_o$ ) oscillate out of phase

You'll notice that the oscillations in these parameters are out of phase with each other, and the oscillations, combined with the phase delays, indicate to us the presence of some sort of regulatory feedback loop.



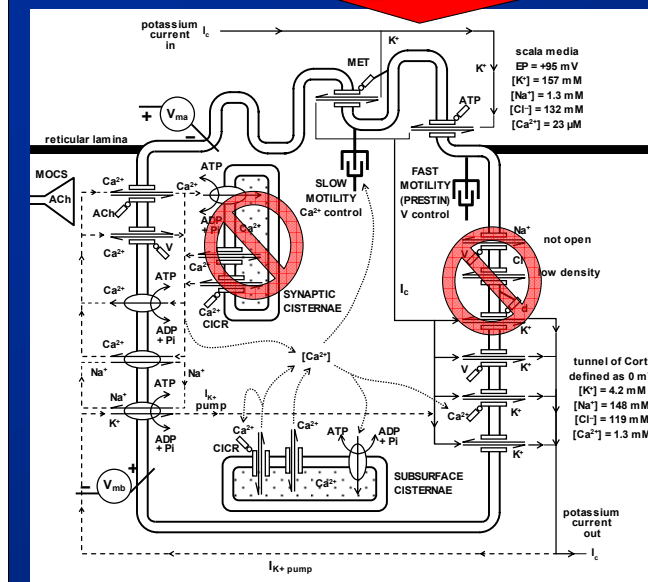
## Slow oscillatory behaviour in the cochlea

Experimentation and mathematical modelling undertaken to examine the possibility that many cochlear oscillations are produced by oscillations in cytosolic calcium concentration.

Now, we developed the outer hair cell model in order to examine the possibility that these very slow oscillations in cochlear gain during the “bounce” and other perturbations are caused by a regulatory feedback loop within the outer hair cell involving **calcium**.

To understand what we mean by this, and how these oscillations could occur, let us look at the membrane transport mechanisms present in the outer hair cell.

## Schematic diagram of OHC cellular components



### Apex

- d-sensitive K<sup>+</sup> channel
- ATP-sensitive cation channels

### Base

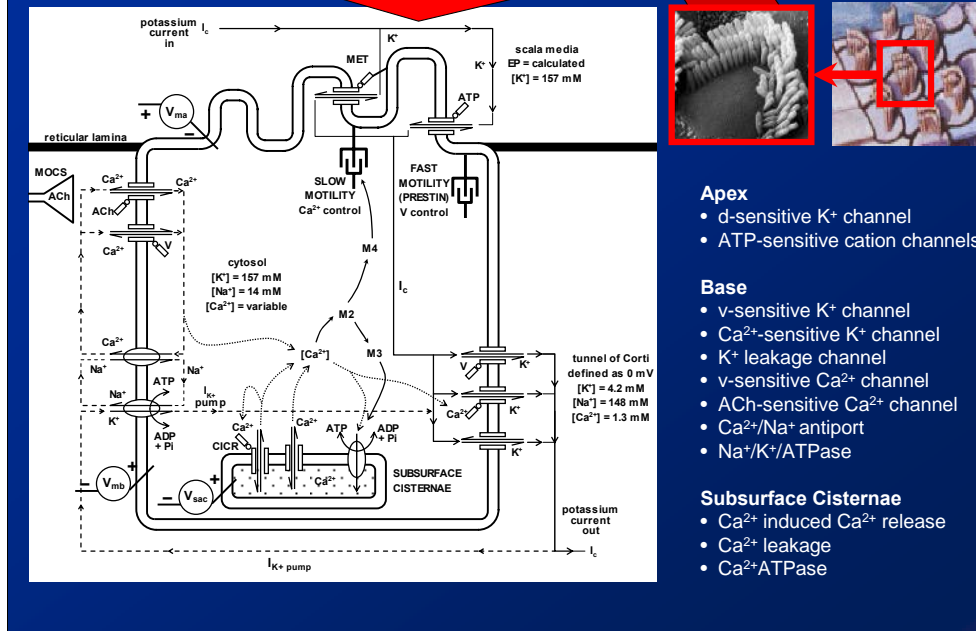
- v-sensitive K<sup>+</sup> channel
- Ca<sup>2+</sup>-sensitive K<sup>+</sup> channel
- K<sup>+</sup> leakage channel
- v-sensitive Ca<sup>2+</sup> channel
- ACh-sensitive Ca<sup>2+</sup> channel
- Ca<sup>2+</sup>/Na<sup>+</sup> antiport
- Na<sup>+</sup>/K<sup>+</sup>/ATPase

### Subsurface/Synaptic Cisternae

- Ca<sup>2+</sup> induced Ca<sup>2+</sup> release
- Ca<sup>2+</sup> leakage
- Ca<sup>2+</sup>/ATPase

This summary diagram shows the channels present in the apical membrane and stereocilia, here, and in the basolateral membrane of the cell, here. Now, to simplify the modelling process we first eliminated some channels which were either not active under physiological conditions, or were of low density, and we also consolidated the synaptic cisternae and subsurface cisternae into one main calcium storage organelle.

## Schematic diagram of OHC model components



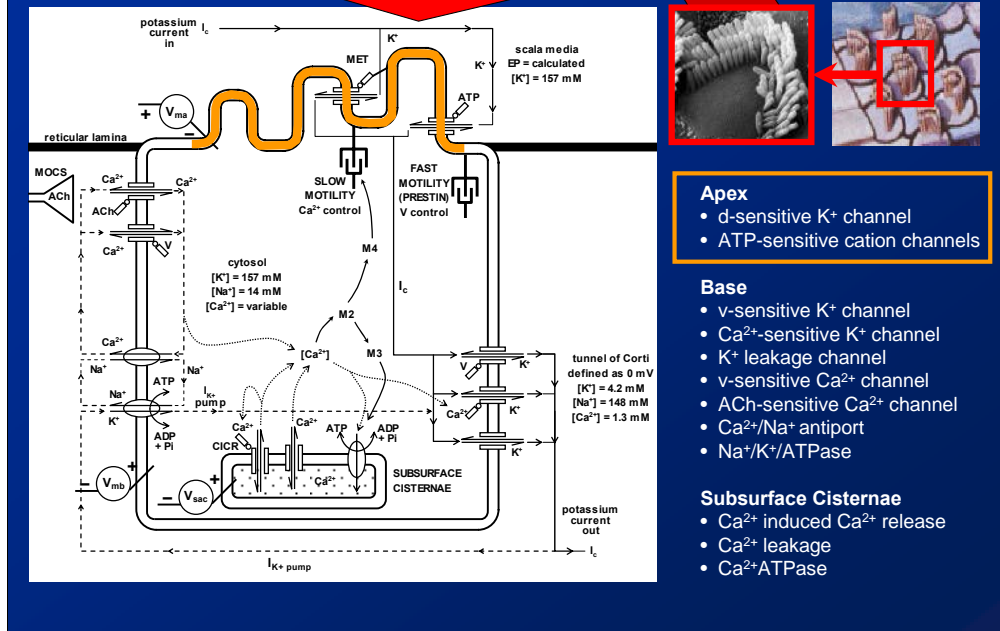
- Apex**
- d-sensitive  $K^+$  channel
  - ATP-sensitive cation channels

- Base**
- v-sensitive  $K^+$  channel
  - $Ca^{2+}$ -sensitive  $K^+$  channel
  - $K^+$  leakage channel
  - v-sensitive  $Ca^{2+}$  channel
  - ACh-sensitive  $Ca^{2+}$  channel
  - $Ca^{2+}/Na^+$  antiport
  - $Na^+/K^+$  ATPase

- Subsurface Cisternae**
- $Ca^{2+}$  induced  $Ca^{2+}$  release
  - $Ca^{2+}$  leakage
  - $Ca^{2+}$  ATPase

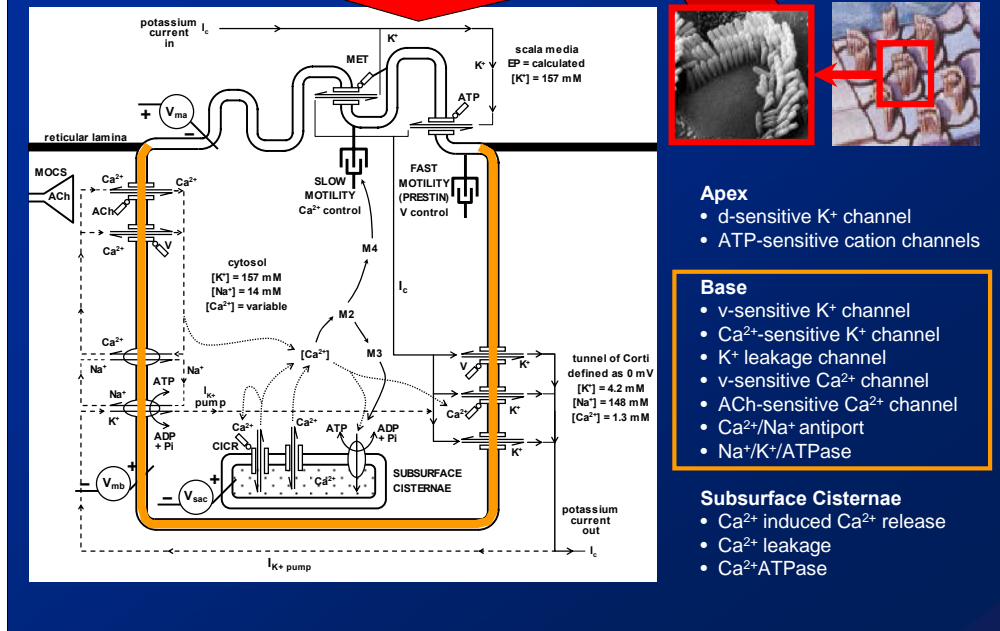
So in the version of the hair cell we modelled...

## Schematic diagram of OHC model components



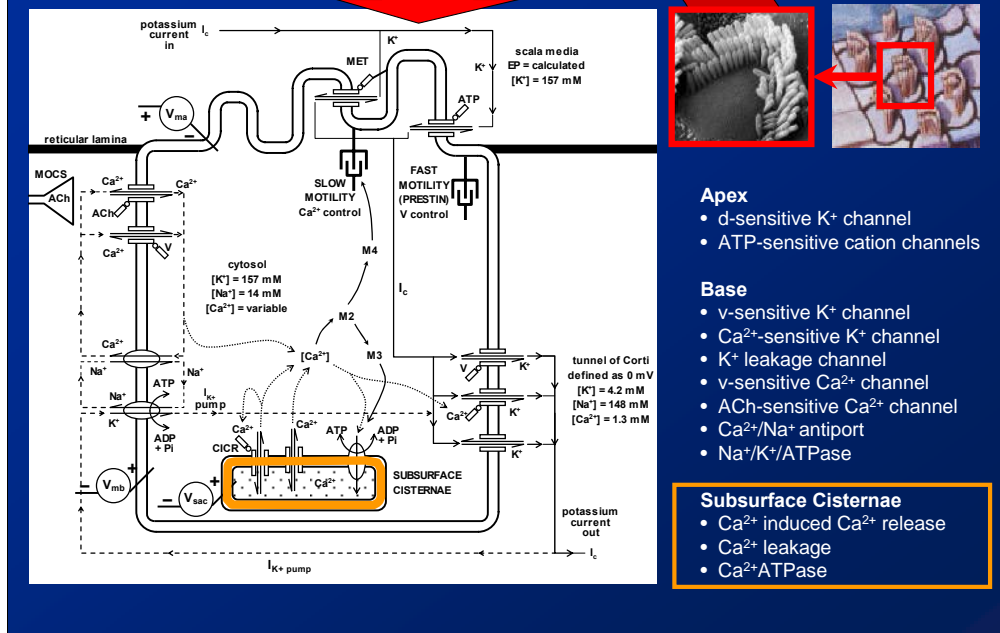
...we have, in the **apical membrane**, the stereocilia with their MET channels and ATP-sensitive cation channels, ...

## Schematic diagram of OHC model components



...while in the **basolateral wall** of the OHC we have a variety of channels transporting potassium, sodium, and calcium.

## Schematic diagram of OHC model components



### Apex

- d-sensitive K<sup>+</sup> channel
- ATP-sensitive cation channels

### Base

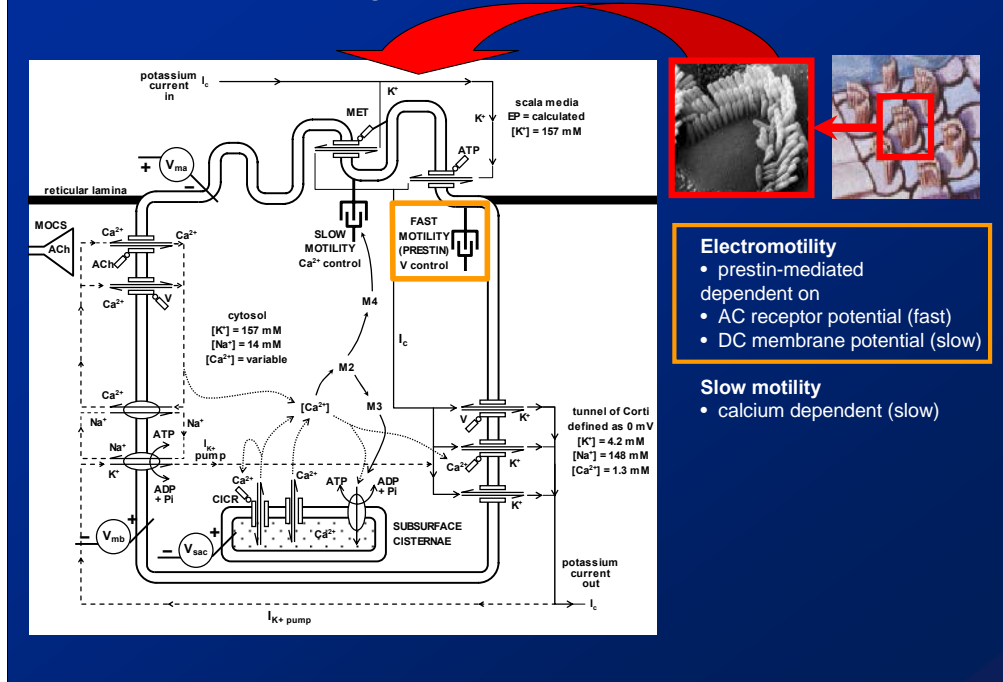
- v-sensitive K<sup>+</sup> channel
- Ca<sup>2+</sup>-sensitive K<sup>+</sup> channel
- K<sup>+</sup> leakage channel
- v-sensitive Ca<sup>2+</sup> channel
- ACh-sensitive Ca<sup>2+</sup> channel
- Ca<sup>2+</sup>/Na<sup>+</sup> antiport
- Na<sup>+</sup>/K<sup>+</sup>/ATPase

### Subsurface Cisternae

- Ca<sup>2+</sup> induced Ca<sup>2+</sup> release
- Ca<sup>2+</sup> leakage
- Ca<sup>2+</sup>ATPase

We also assume mechanisms for the transport of calcium into and out of the **subsurface cisternae**, or lateral sacs.

## Schematic diagram of OHC model components

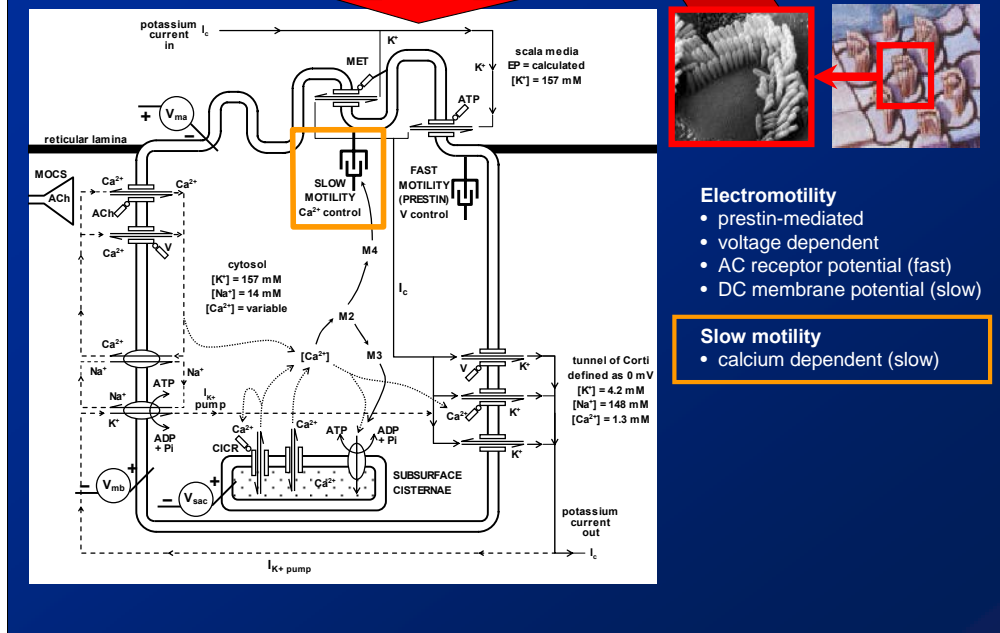


- Electromotility**
- prestin-mediated dependent on
  - AC receptor potential (fast)
  - DC membrane potential (slow)

- Slow motility**
- calcium dependent (slow)

Also shown in this diagram are the two somatic motility mechanisms. We didn't include motility arising from the stereocilia. We have the **prestina-mediated electromotility** in the lateral membrane of the cell. Not only is this electromotility responsible for the cycle-by-cycle amplification in the active process, but it is also capable of acting in a slow, graded manner, to produce length changes in response to changes in DC membrane potential. This was referred to by Frolenkov as "activating fast electromotility slowly".

## Schematic diagram of OHC model components



### Electromotility

- prestin-mediated
- voltage dependent
- AC receptor potential (fast)
- DC membrane potential (slow)

### Slow motility

- calcium dependent (slow)

We also have calcium-dependent slow motility, whereby changes in cytosolic calcium concentration cause a modulation of axial stiffness of the outer hair cells and reorganisation of the cytoskeleton, to produce a **slow length change** of the cell.



## Importance of cytosolic calcium

### Calcium control of transducer operating point

- via slow motility
- Therefore:
  - Apical permeability
  - DC membrane potential

### Calcium control of basolateral permeability

- via  $\text{Ca}^{2+}$ -sensitive  $\text{K}^+$  channels
- Therefore:
  - DC membrane potential
    - slow electromotility
  - AC receptor potential
    - fast electromotility
    - cochlear gain

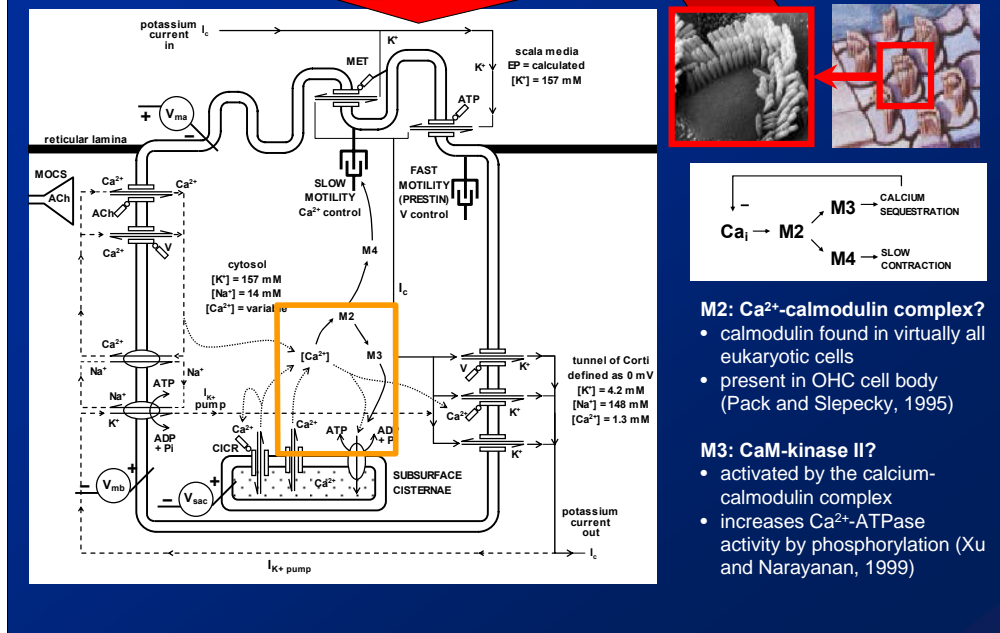
### Calcium control of calcium itself

So, because of the slow-motility mechanism, calcium is able to control the operating point of the OHC, which changes the permeability of the apical membrane of the hair cell via the MET channels, and therefore changes the hair cell membrane potential.

Increases in calcium also cause the opening of the SK-type potassium channels, increasing the permeability of the basolateral wall of the OHC. This permeability also determines the **basolateral membrane potential** of the OHC, the **standing current** through the OHCs, and, in the presence of sound, determines the magnitude of the AC receptor current and receptor potential. Therefore, an increase in cytosolic calcium increases the basolateral permeability and decreases the amplitude of the AC receptor potential required to drive somatic electromotility, resulting in a hearing loss.

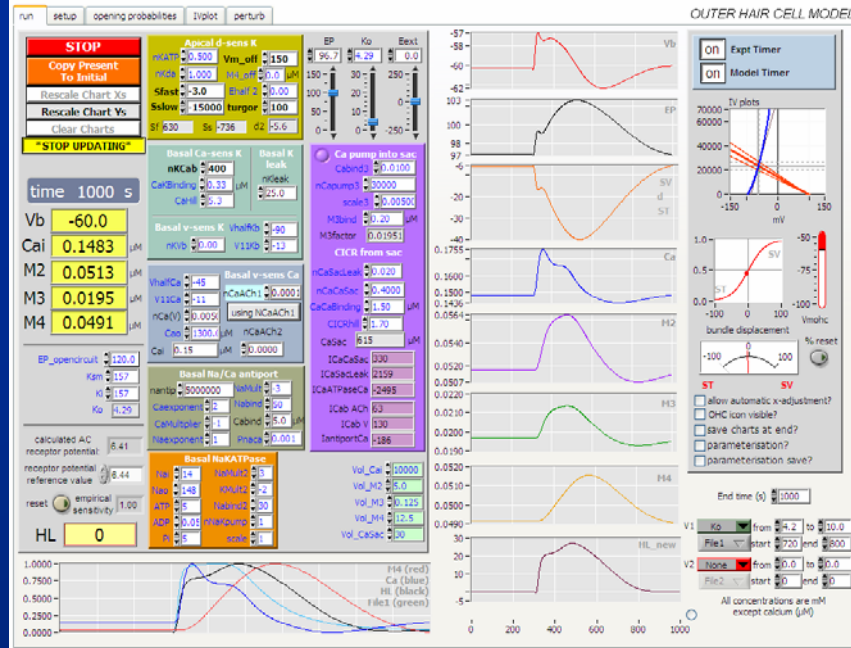
Not only does calcium regulate operating point and basolateral permeability, it also controls the level of calcium itself, and this, we believe, allows the calcium concentration to oscillate.

## Schematic diagram of OHC model components



To provide the phase delays required for this oscillation, we've assumed that the extrusion or sequestration of calcium occurs at the end of a second messenger cascade involving two intermediates, M2 and M3, which may correspond to the calcium-calmodulin complex and CaM-kinase II, respectively.

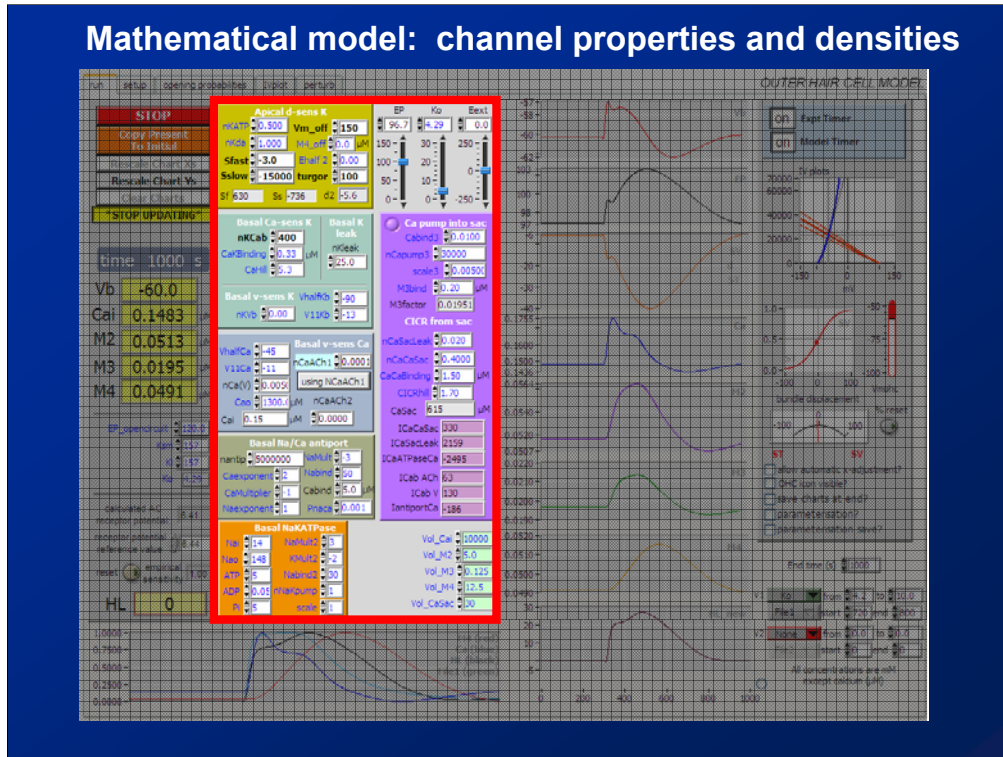
## Mathematical model: front panel display and controls



We created this mathematical model to enable us to set up a virtual hair cell, with relevant transport equations governing each cellular component, and with ionic fluxes integrating to give us concentrations. The model is defined by transport equations such as the Goldman-Hodgkin-Katz (or GHK) equations for 12 different ion channels, each of which contains a number of parameters.

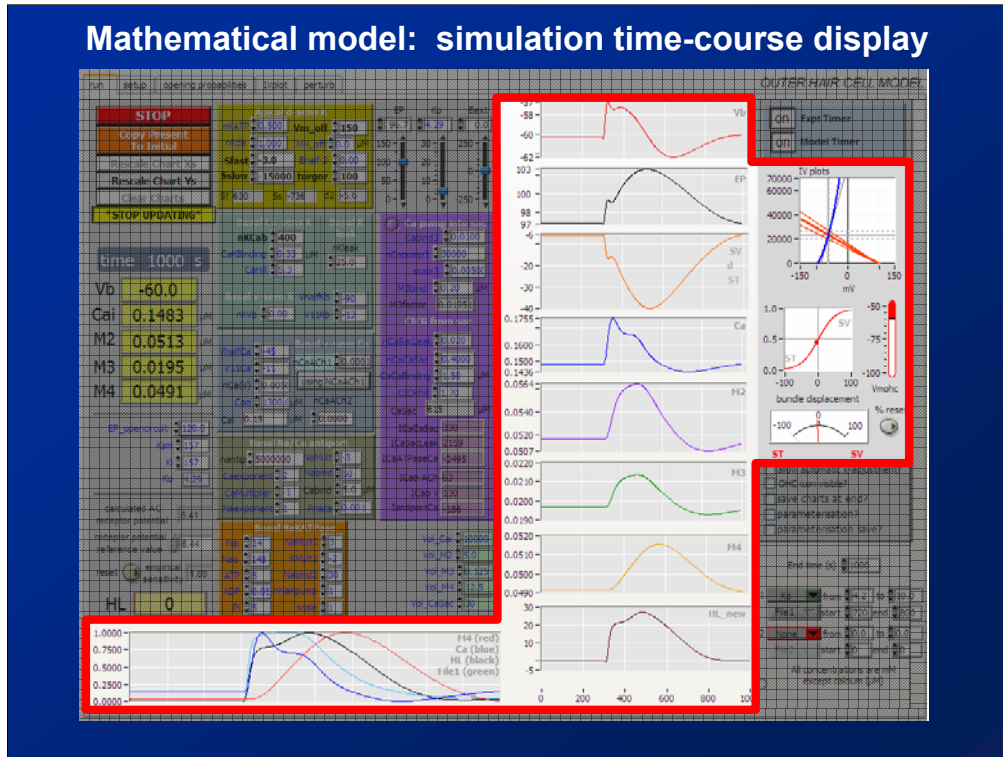
This is the user interface for the model, which was written using LabVIEW. On this screen we have...

## Mathematical model: channel properties and densities



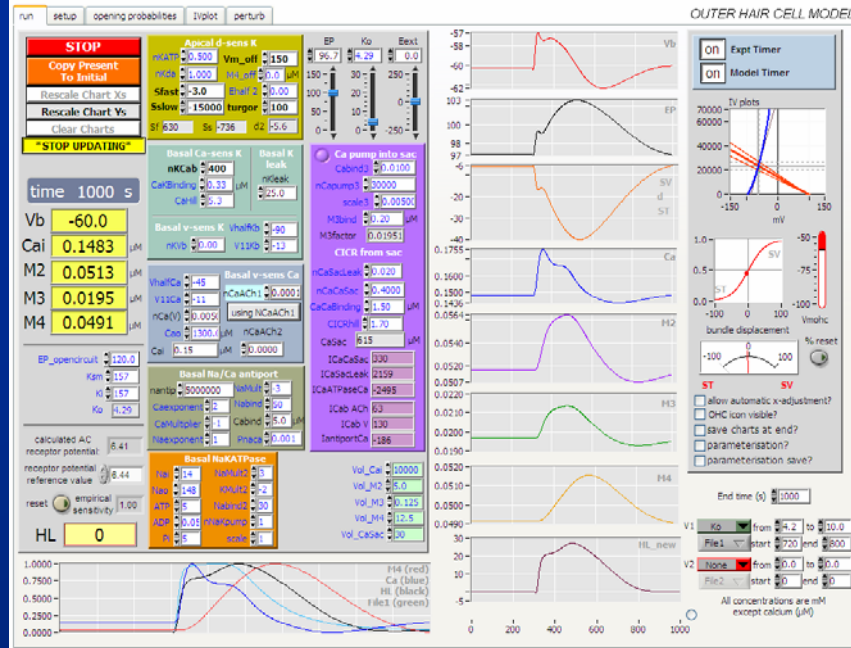
... the main parameters controlling the twelve channels and pumps, ...

## Mathematical model: simulation time-course display



...and the primary output from the model, which was the time-course of the changes in the membrane potential, EP, operating point, calcium and second-messenger concentrations, and the predicted outer hair cell hearing loss during our simulated perturbations.

## Mathematical model: front panel display and controls



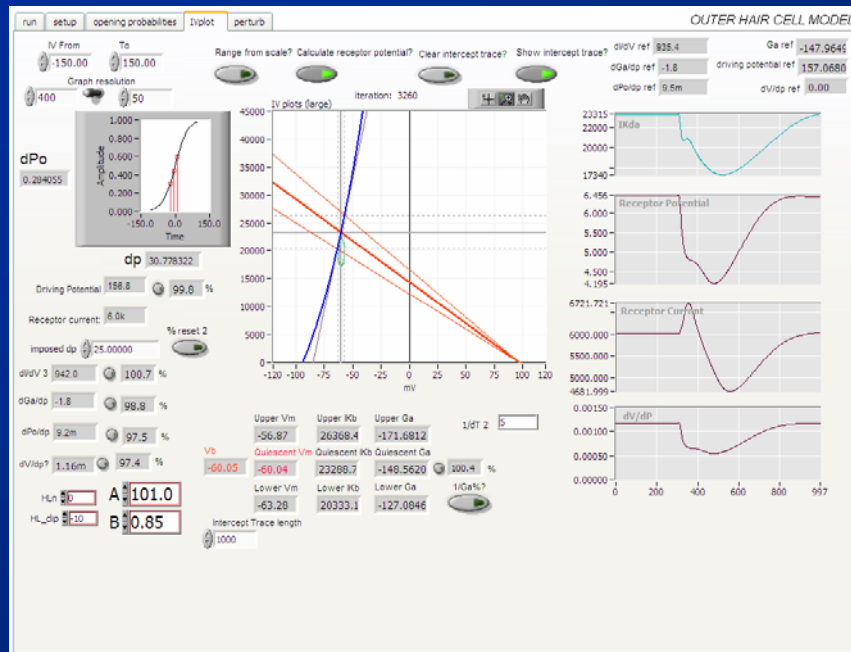
The simplest perturbations were step-changes in particular parameters, such as for DC current injection we have a step-change in the open-circuit EP, but for more complicated perturbations...

## Mathematical model: experimental perturbations



...time-courses for the changes in parameters could be imported from text files. For example, to simulate perilymphatic perfusions of elevated potassium, the time-course of the predicted changes in perfusate concentration at a particular location in the cochlea could be imported from the Alec Salt's Cochlear Fluids Simulator, and this parameter would then change dynamically and smoothly over time during the simulation. Similarly, a low-frequency tone can be imported and used to move the stereocilia back and forth.

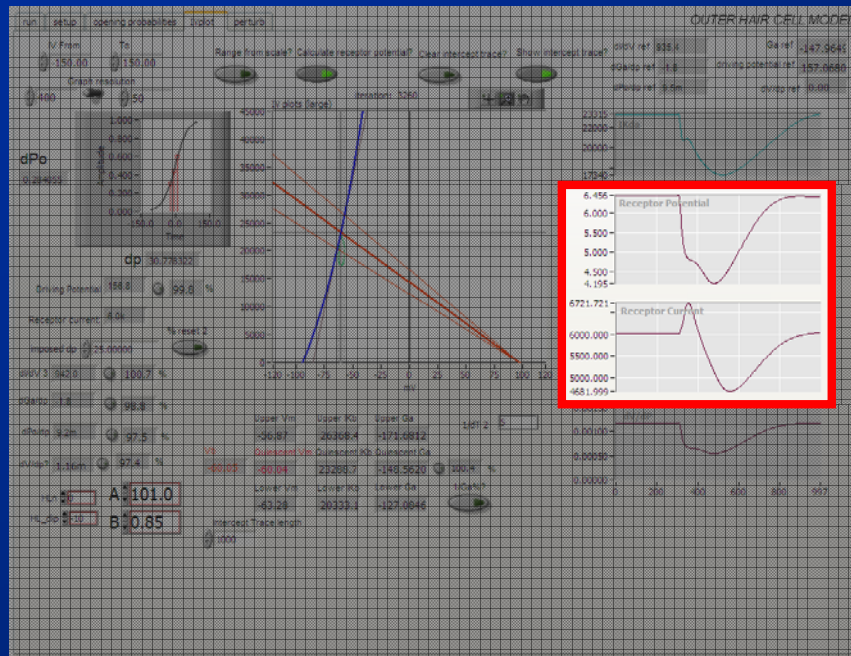
## Mathematical model: IV plot and load-line analysis



The second main output of the mathematical model was the IV-curve section, shown here, ...

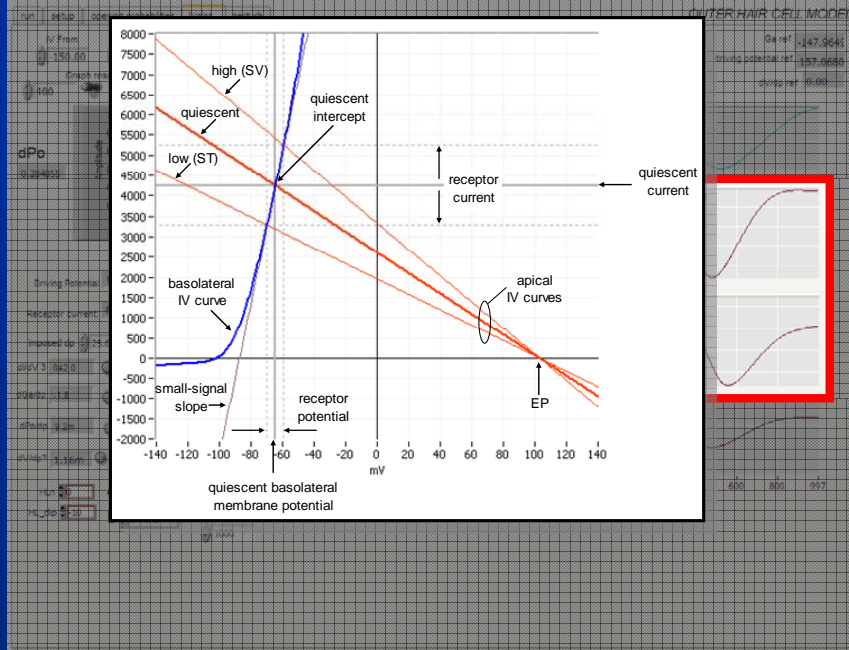


## Mathematical model: IV plot and load-line analysis



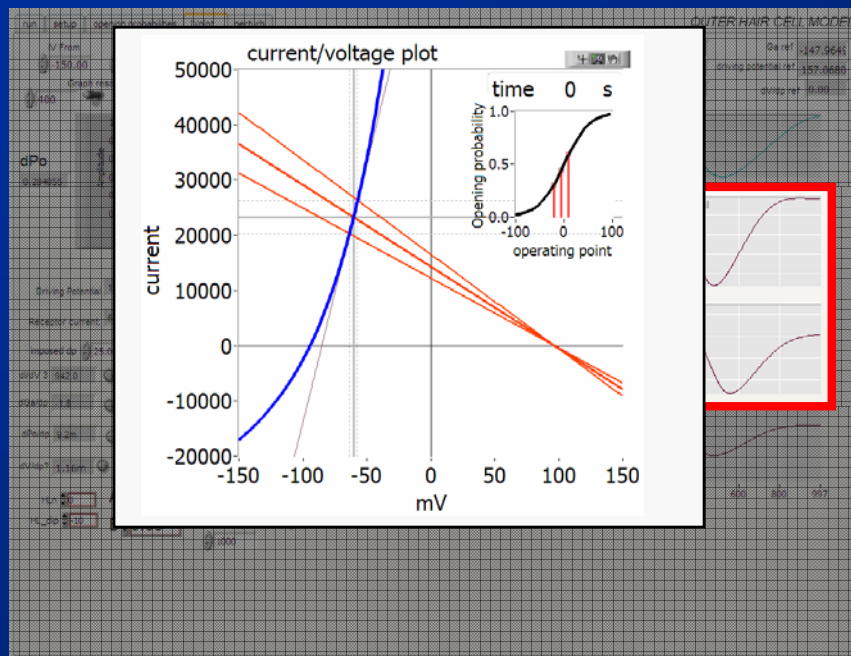
...which allowed us to calculate the AC receptor current and receptor potential...

## Mathematical model: IV plot and load-line analysis



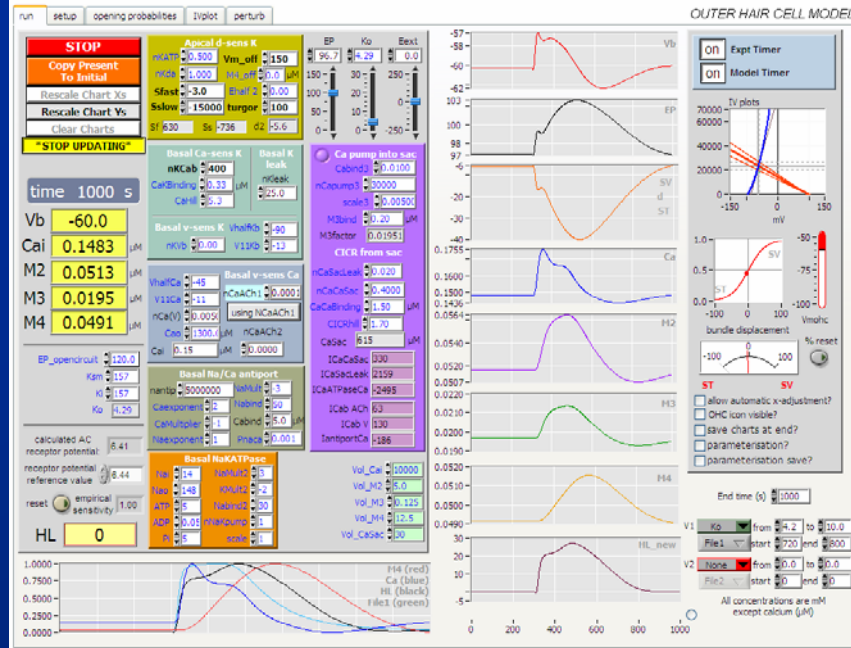
...using load-line analysis.

## Mathematical model: IV plot and load-line analysis



This section of the display provided a valuable visual tool for getting a handle on the functioning of the model, as you can see the IV-characteristics change in a very dynamic manner during perturbations, such as during the perfusion of artificial perilymph containing an elevated potassium concentration, shown here.

## Mathematical model: front panel display and controls



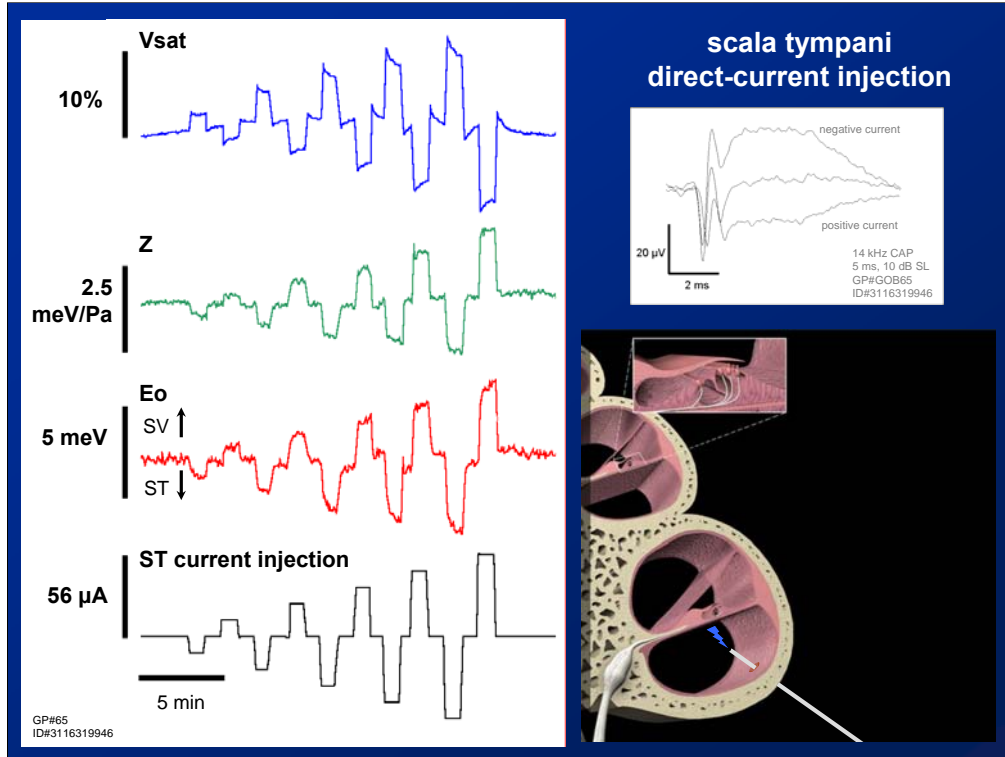
I can provide more details about the model itself to those who are interested afterwards, but in the remaining time I have left I am going to present some example *results* from the model.

Over a period of several years, the results from the model were repeatedly compared with the results of guinea-pig experiments, with the aim of settling a **single set of model parameters** that provided the best fit to the results from many different perturbations, and these are essentially the numbers that you see here.

## Experiments:

1. direct-current injection into scala tympani;
2. exposure to intense low-frequency tones.

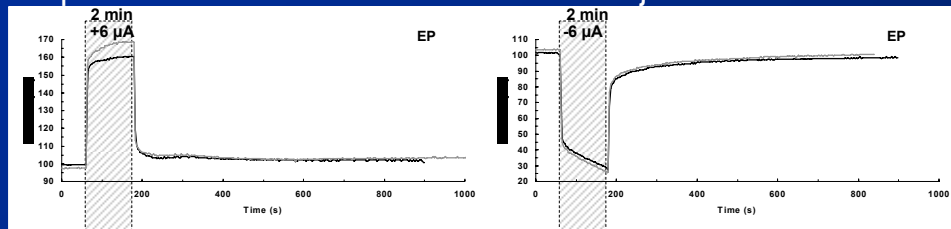
Using this standard parameter set, the model was capable of reproducing many key aspects of our experimental data, and I'd like to show you some examples of that now. It's important to note that there were other aspects of the results the model *could not* reproduce, and I'll discuss those shortly.



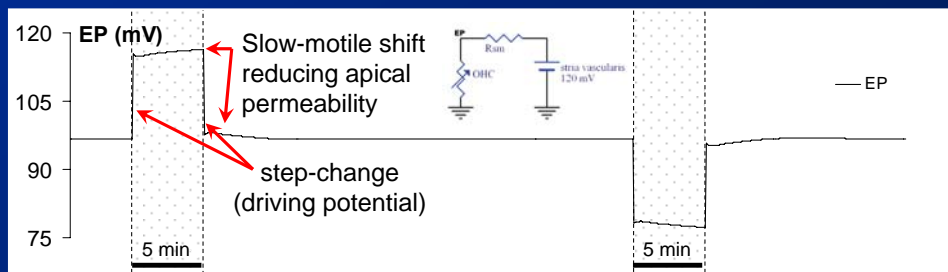
One of the experimental results we set out to model was the changes in the Boltzmann parameters during the injection of DC current into scala tympani and scala media.

## Example results from mathematical model

Experimental data: scala media current injection



Model results (using standard set of parameters):

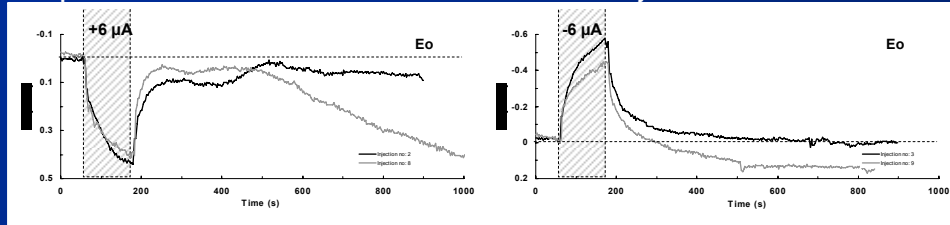


In this top panel, we have experimental data from the guinea pig, and in the bottom panel we have the simulation results for a similar perturbation in our mathematical model.

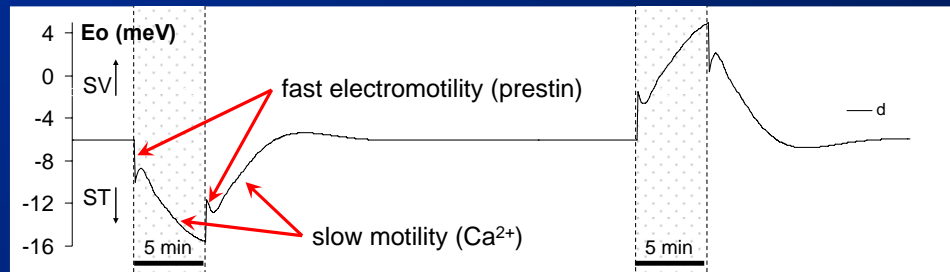
Now, the perturbation we put into the model was the step changes in EP here and here, but the model reproduces the changes in EP over the duration of the current injection, and after the offset of the injection here. These slow changes in the EP in the model were due to the influx of calcium through voltage-gated calcium channels causing a slow-motile contraction of the cell towards scala tympani, reducing the shunt through apical conductance and therefore increasing the EP.

## Example results from mathematical model

### Experimental data: scala media current injection



### Model results (using standard set of parameters):



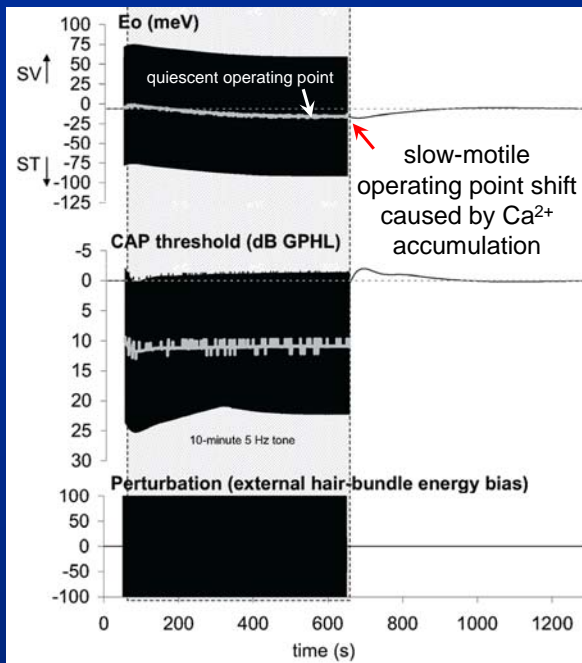
We can see the operating point changes during current injection here. So, remember, this is our measure of resting hair-bundle angle, or level of hair cell contraction. We see the increased driving potential causing a step-depolarisation and fast-motile contraction, which was followed by a further slow-motile contraction due to the influx of calcium. You can see that there are a few bumps and wiggles, but that the fast and slow components were reasonably well replicated here.



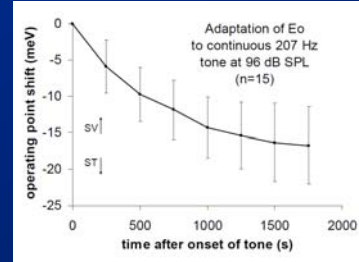
**Low-frequency exposure:**

Now let us examine the results of the model for exposure to a low-frequency tone.

## Low-frequency exposure: Model results (std. parameters)



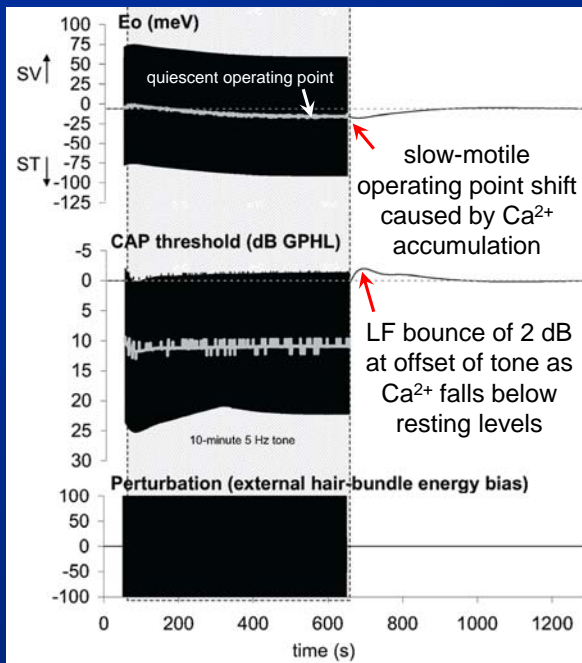
Experimental data:  
(Marcon & Patuzzi, 1995)



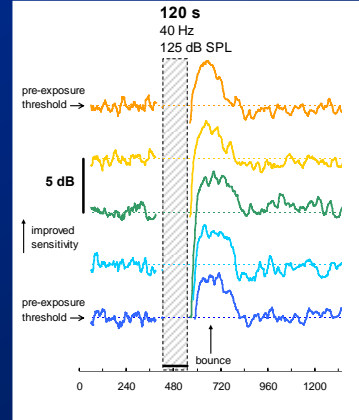
(see also Salt, 2004)

Using the same set of model parameters – the single set were homed in on - the model was capable of reproducing the slow movement of the operating point towards scala tympani that we commonly observe during a low-frequency tone. It also reproduced the changes in the EP over this period (which I'll show in a moment), and...

## Low-frequency exposure: Model results (std. parameters)

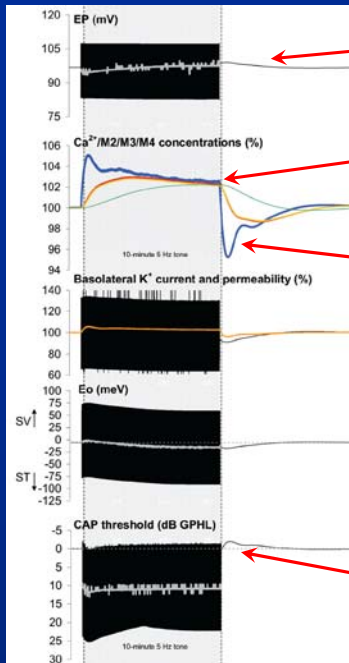


Experimental data:  
(O'Beirne, 2005)



...also mimicked the transient hypersensitivity we see following the offset of low-frequency exposure – known as the “bounce”. In this case, we are assuming that the influx of calcium into the cell during the low-frequency stimulation causes the levels of the second messengers, M2 and M3, to integrate up and increase the rate of removal of calcium from the cell, so that...

## Low-frequency exposure: Model results (std. parameters)



Low basolateral permeability decreases  $K^+$  shunt, increasing EP and causing transient tinnitus

Presence of LF tone causes cytosolic  $Ca^{2+}$  to rise, which causes a slow increase in M3 activity, which accelerates  $Ca^{2+}$  sequestration

$Ca^{2+}$  entry stops but its removal continues, causing  $Ca^{2+}$  levels to fall to 4.5% below control levels

LF bounce of 2 dB at offset of tone as  $Ca^{2+}$  falls below resting levels

...at the offset of the tone, the entry of calcium due to the tone stops, but the removal of calcium continues for a while, causing its levels to fall below resting values. This decrease in calcium level **reduces** the basolateral permeability and **increases** the AC receptor potential driving prestin, thereby increasing sensitivity. The low basolateral permeability also reduces the shunt through the OHCs, thereby increasing the EP and causing one type of peripheral tinnitus.

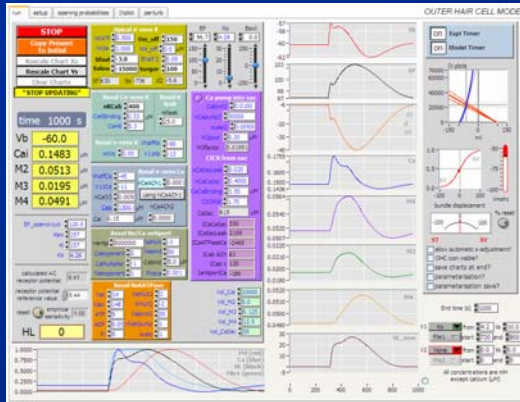
## Conclusions

- While the model accounts for many key features of the data, several model predictions are not consistent with experimental results
- Data more consistent with functional separation of intracellular calcium into **two pools**
  - one controlling basolateral permeability
  - one controlling slow motility
- Modelling continuing with this “two-pool” version

So, as I discussed earlier, the process of designing and programming the model, and then testing it experimentally, has taken several years. However, after many experiments and iterations of the modelling process, there were a number of key results which the model was simply incapable of replicating. But rather than indicating that further fine-tuning of the mathematical model was required, these “exceptions” to the model indicated that some more basic, more fundamental, changes to our schematic model of the OHC were required to fully account for the observed experimental behaviours.

I don't have enough time to go into it in any detail, but we have come to the realisation that a number of these discrepancies between the simulation results and the experimental data can be resolved if we model the cytosolic calcium in two distinct pools: one which controls basolateral permeability, but does not have access to the slow-motile machinery, and one which controls slow-motility, but does not have access to the sodium/calcium antiport, or calcium-sensitive potassium channels controlling basolateral permeability. This, for example, would account for the lack of a significant operating point shift during efferent stimulation (which we assume would affect only the basolateral permeability pool), and it provides a better account of the operating point shifts we observe during perfusions of low-sodium artificial perilymph.

# Acknowledgements:



I'd like to thank

Dr. Robert Patuzzi  
Mr. Daniel Brown  
Dr. Catherine McMahon  
Dr. Simon Marcon  
Mr. Neil Wareing

and other colleagues from the Auditory Laboratory,  
Physiology, University of Western Australia.

I'd like to thank...